Performance Analysis of Individual and Combined Quality Effects for Iris Biometrics

by Natalia Schmid

Participants: Nathan Kalka (GRA), Jinyu Zuo (GRA), Dr. Bojan Cukic

Lane Department of Computer Science and Electrical Engineering
West Virginia University

Motivation

Despite what is published in the literature, there is **no concept of panacea** iris biometric.

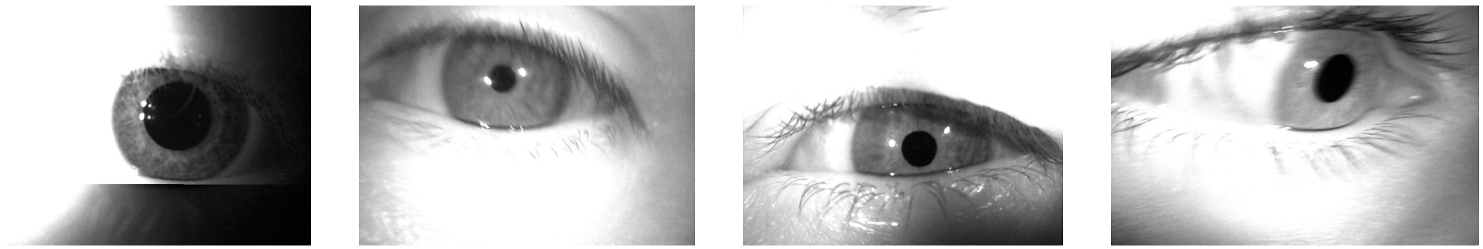

Images from an OKI camera collected at WVU

Sources of noise:

- Irregular Lighting
- Smear due to movement of camera or user
- Bad camera focus
- Physiology of the eye (Convexity of iris surface; Natural position and geometry of the eye)
- CCD shot noise

Motivation: Segmentation

Our implementation of Daugman's Method

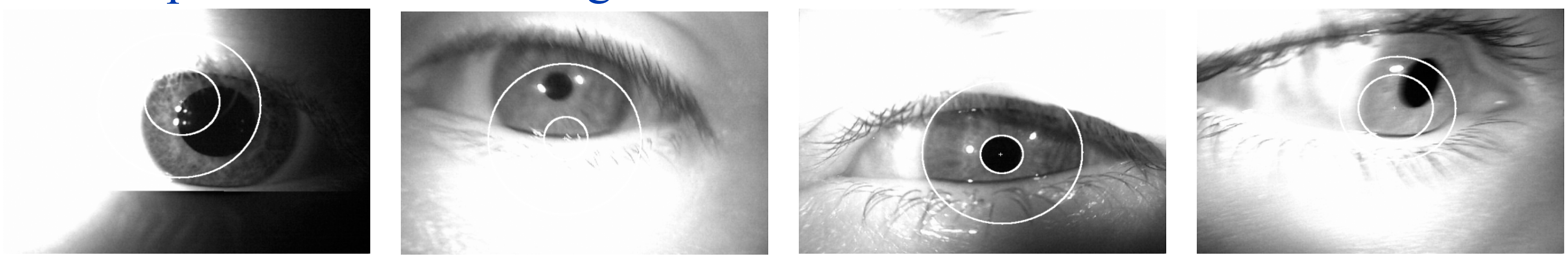

Morphological Operators

Our implementation of Wildes' segmentation algorithm.

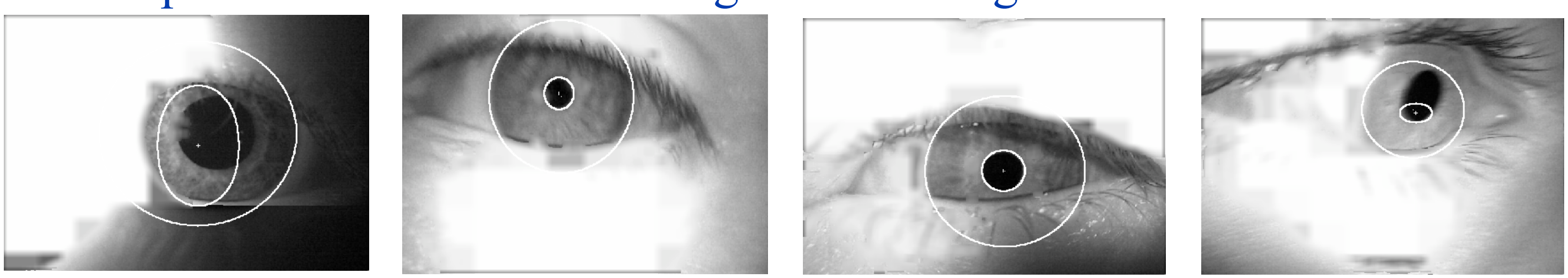

Motivation: Synthetic Studies

Purpose:

- To evaluate the effect of noise factors on performance using Gabor based, PCA, and ICA encoding techniques.
- Gain insight to factor estimation.

Procedure:

- 40 good quality images were selected from CASIA and WVU datasets (10 users for each dataset, 2 images per user) based on visual evaluation.
- One template per user was synthetically degraded at different strengths and processed using our implementation of Daugman's algorithm.
- Templates of degraded images were compared against non-degraded templates using Hamming distance, and Euclidean distance metrics.

Defocus Blur

- May result from many sources
- The main source the focal point is outside the depth of field
- To simulate use Gaussian filters

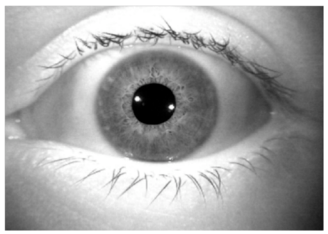
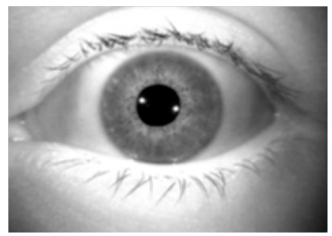
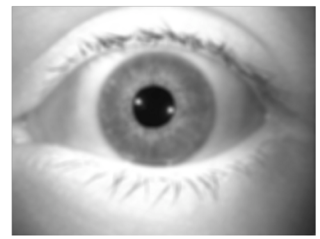

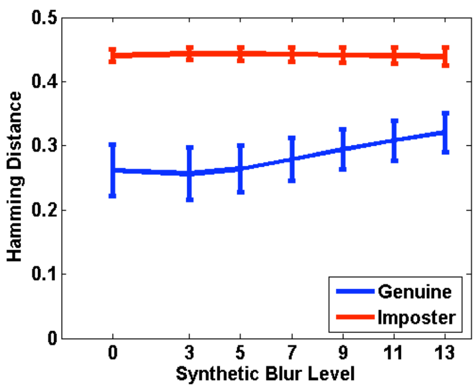

Gabor-based

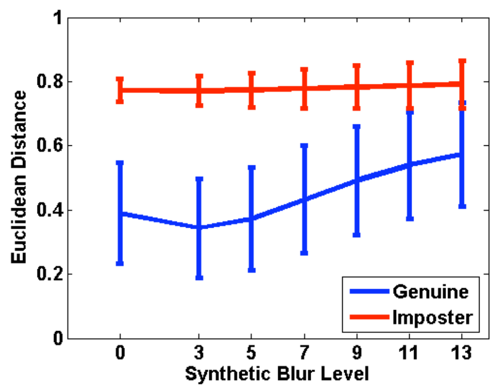

Global PCA

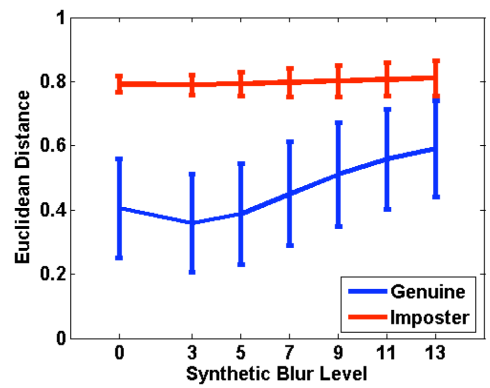

Global ICA

Motion Blur

- Linear and non-linear motion blur We consider only linear motion blur.
- Two parameter model: direction and pixel-smear.

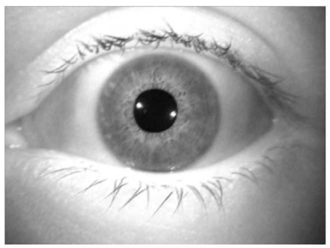

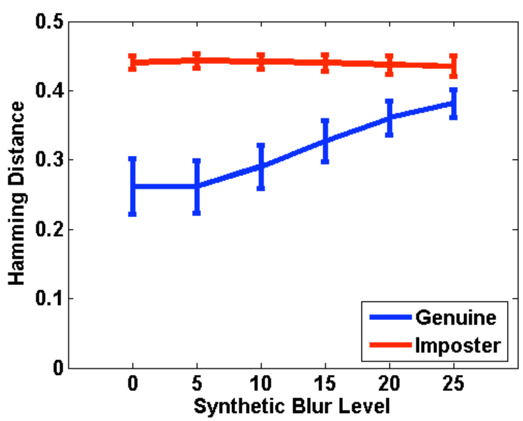

Gabor-based

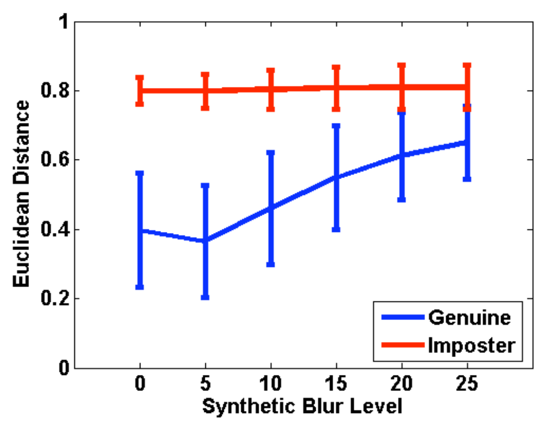

Global PCA

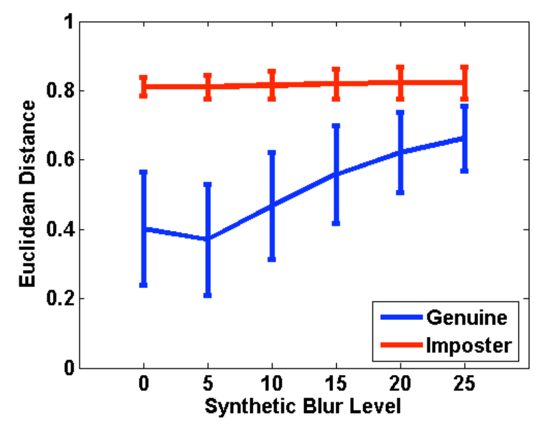

Global ICA

Off-Angle

- Non-cooperative users or Iris at a distance
- Evaluate performance using 36 iris classes from the WVU off-angle iris image database. Database has 208 iris classes, 4 images per each class (two from frontal views, 15 degree view, and 30 degree view)

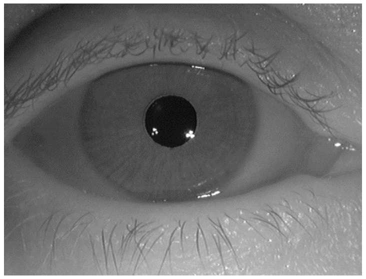

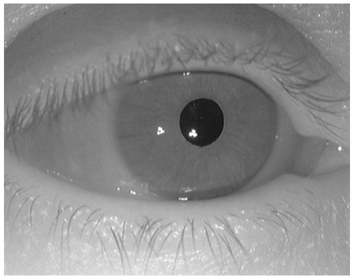

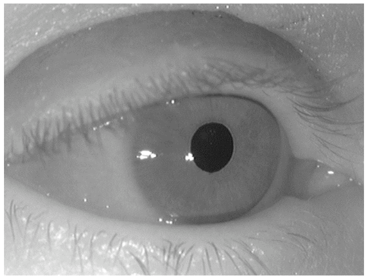

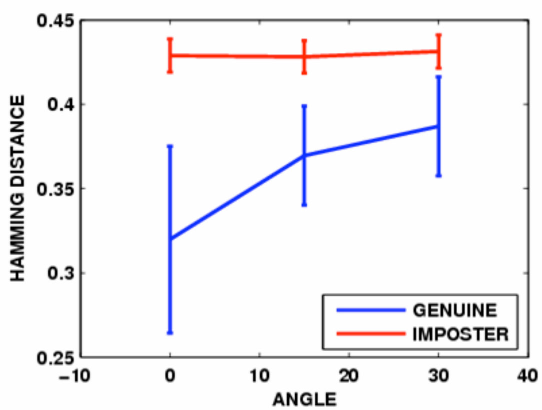

Gabor-based

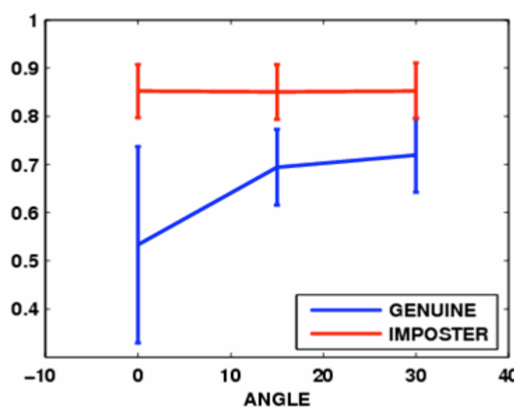

Global PCA

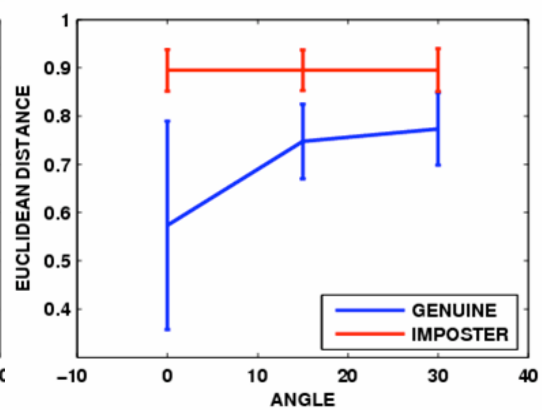

Global ICA

Pixel Counts

- Downsample the normalized iris image at varying scales

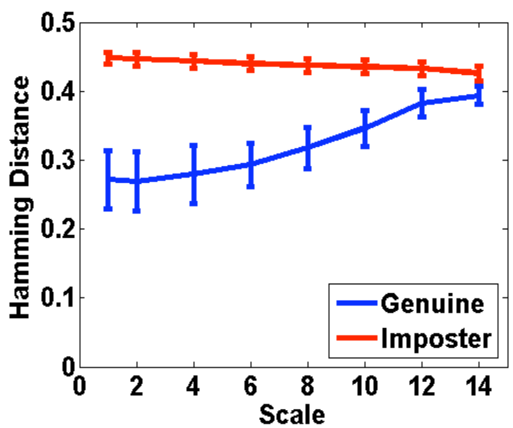

Gabor-based

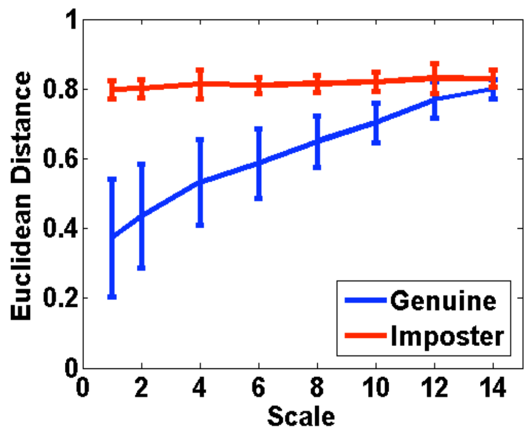

Global PCA

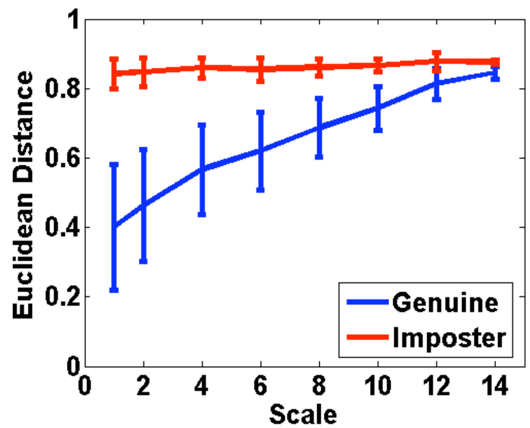

Global ICA

Objective

Design quality assessment tool

- that allows adaptive recognition system
- that provides online feedback regarding image quality (fast feedback).

Factors:

- Defocus Blur
- Motion Blur
- Off-Angle
- Lighting
- Occlusion
- Specular Reflection
- Pixel Counts

Previous Works

- **(Zhu et al. 2004)** - evaluate quality by analyzing the coefficients of particular areas of iris texture by employing discrete wavelet decomposition.
- **(Chen et al. 2006)** - Classify iris quality by measuring the energy of concentric iris bands obtained using 2-D wavelets.
- **(Zhang and Salganicaff 1999)** - examine the sharpness of the region between the pupil and the iris.
- **(Ma et al. 2003)** - analyze the Fourier spectra of local iris regions to characterize defocus, motion and occlusion.
- **(Daugman 2004) and (Kang and Park 2005)** - characterize quality by quantifying the energy of high spatial frequencies over the entire image region.

Features of Previous Works:

- Estimation of a single or pair of factors such as defocus, motion blur, and occlusion
- Require complete segmentation

Estimation: Defocus

- Defocus attenuates mid-high frequency content.
- Explore High pass filtering to evaluate High frequency content **globally** as well as **locally**

$$100*\frac{x^2}{x^2+c^2} \Rightarrow \frac{x^2}{x^2+P^2}$$

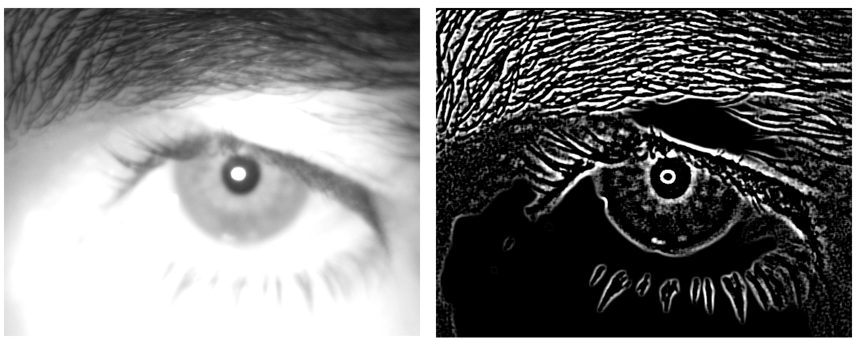

Focus=0.91

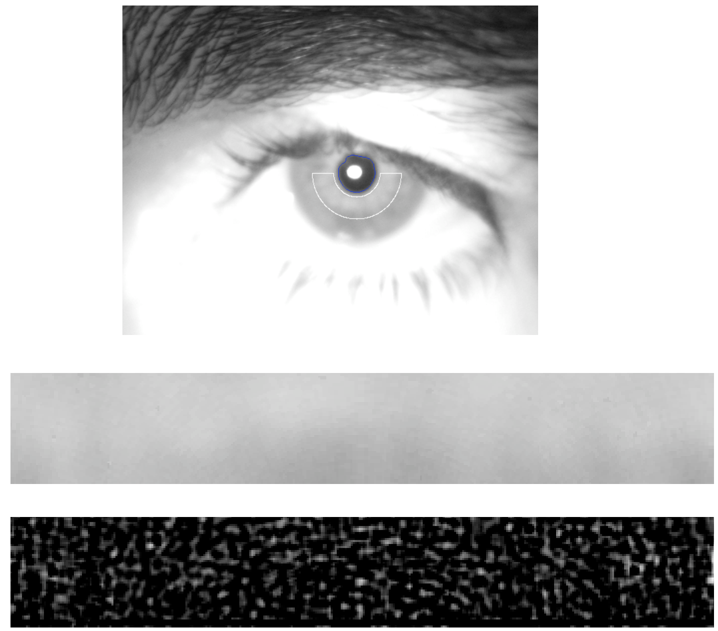

Focus=0.31

J. Daugman, “How Iris Recognition Works,” IEEE Trans. Circuits and Systems Video Technology, vol. 14, no. 1, Jan. 2004.

Estimation: Motion Blur

- Need to estimate **angle** and **smear** level.
- Use Fourier analysis (angle can be estimated from logarithmic transformation of the magnitude)

Example:

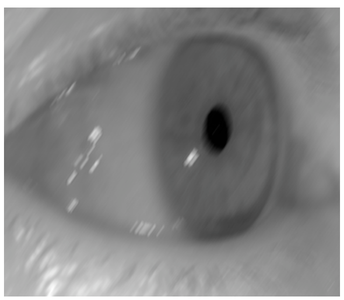

Motion Blur (45º)

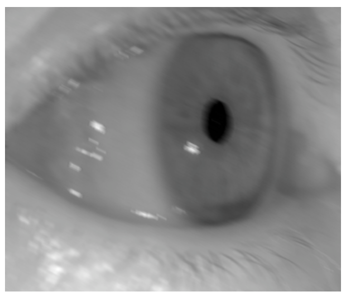

Motion Blur (160º)

Log Magnitude Representation

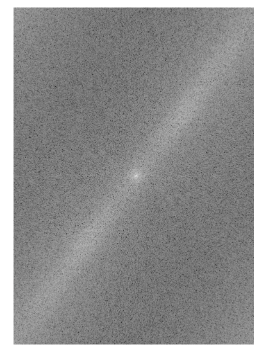

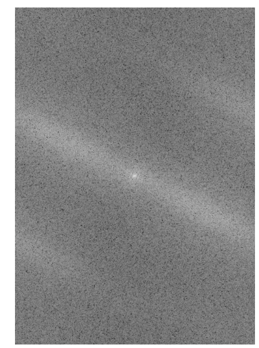

Estimation: Motion

(Smear Level=10, Angle=45)

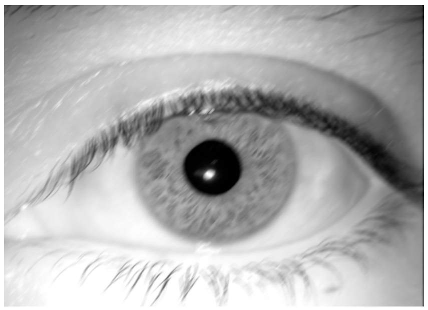

Magnitude of FT

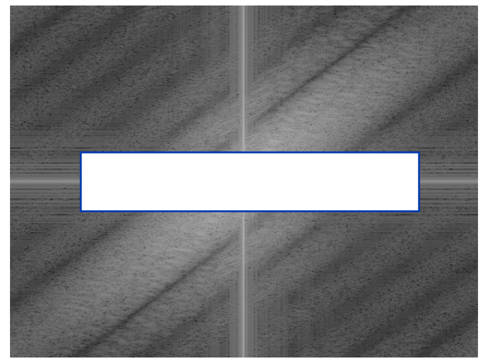

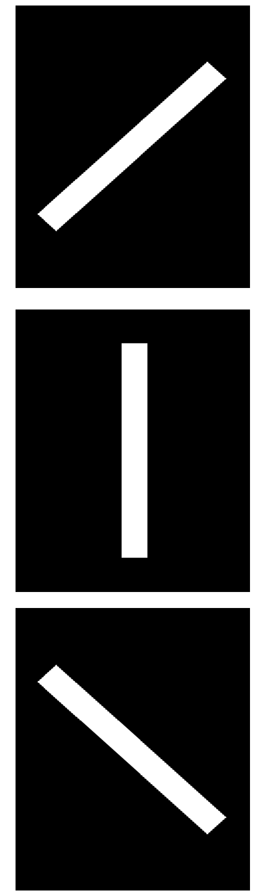

Filter Bank

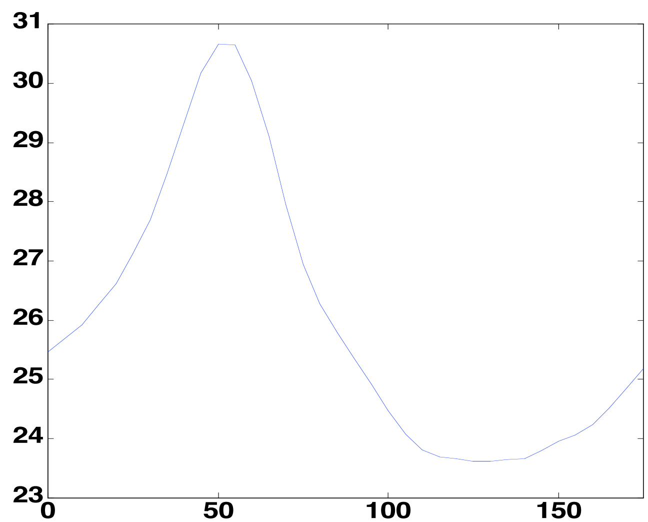

Estimation: Motion

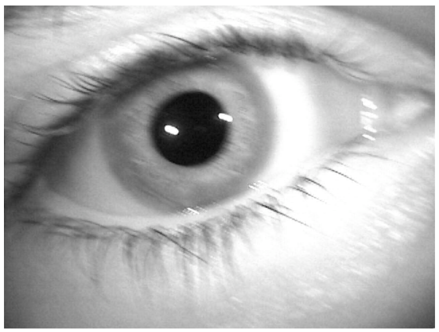

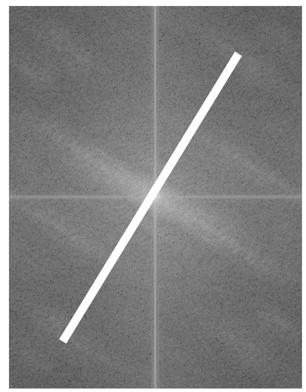

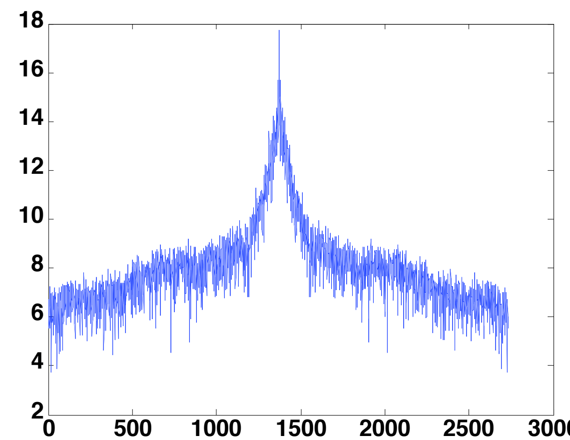

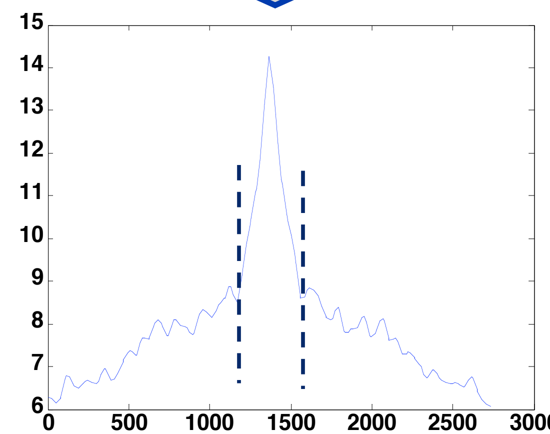

- Once central lobe points are located, the power contained within the width can be calculated.
- The power is then normalized between [0,1].

Estimation: Off-Angle

- WVU dataset of off-angle iris images (208 iris classes, 4 images per class)
- Maximum of integro-differential operator is exhaustively calculated over a range of angles for pitch and role.

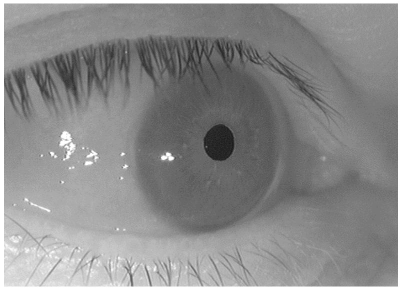

(a) 30 degree image

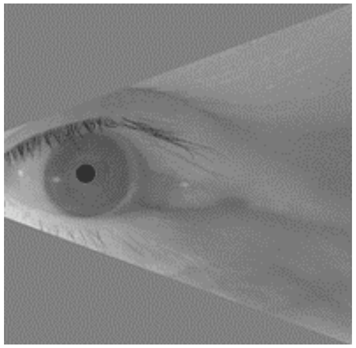

(b) Rectified image

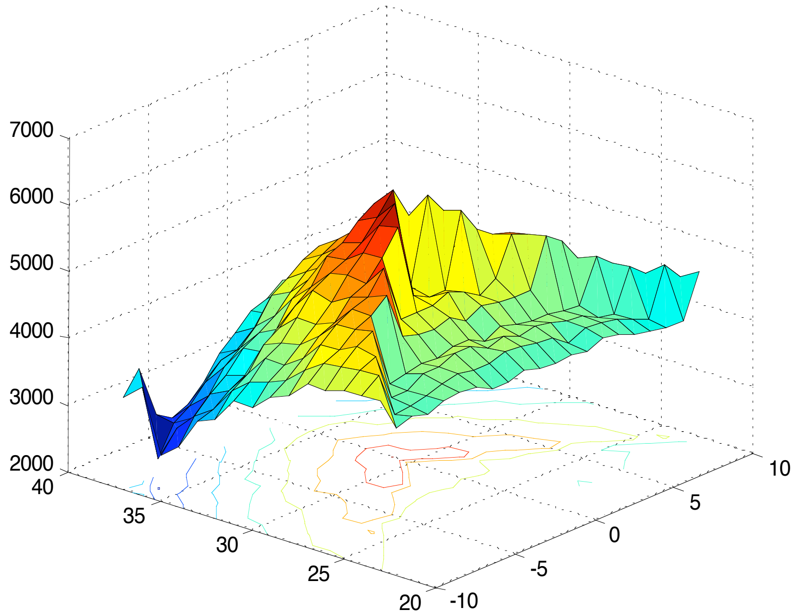

(c) Value of objective function for various angles

Estimation: Occlusion

Use assumption that the sclera region and eyelid region are of differing intensities. Adopt a gradient based approach to finding the edges of upper an lower eyelid occlusion on a "stretched" normalized iris image. To include portions of the sclera in the normalized image, we expand it by approximately 1.1 times the size of the estimated iris radius.

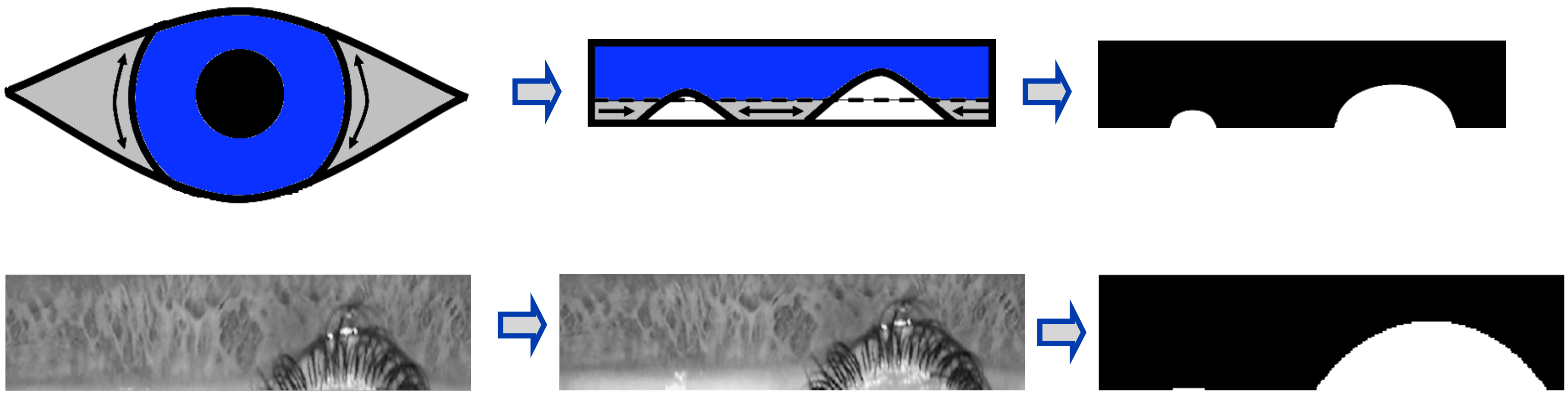

Estimation: Lighting, Specular and Pixel Counts

Specular

- The factor is estimated by hard thresholding. Based on evaluation of CASIA and WVU datasets, a threshold of 240 gives good results.

Lighting

- After estimating occlusions from eyelids and specular, the remaining un-occluded iris portion is split into four regions. The mean in each region is calculated and the variance of the means is used for our estimate of lighting.

Pixel Counts

$$Pcounts = \frac{x_{Estimated}}{x_{Estimated} + x_{Occluded}}$$

Fusion: Dempster-Shafer Approach

- Based on evidential reasoning (belief functions).
- Applications: artificial intelligence, software engineering, and pattern classification.

Dempster's Rule of Combination

- Calculated as the orthogonal combination of all belief functions that are from the same source. The result is a new belief function.

Propositions (Events)

A and B – Image Quality is Bad and Good (our belief), respectively

Fusion: Dempster Shafer

Consider 3 beliefs (Estimated factors) A1, A2, A3 such that $A1 \leq A2 \leq A3$ then min confidence can be calculated by the following expression:

$$M(A1\ ,\ A2) = \frac{(A1 * A2)^n}{(A1 * A2)^n + (1 - A1)^n\,(1 - A2)^n}$$

n ~ correlation

$$M(\,M(A1\ ,\ A2)\ ,\ A3) = \frac{(M(A1\ ,\ A2) * A3)^n}{(M(A1\ ,\ A2) * A3)^n + (1 - M(A1\ ,\ A2)\,)^n\,(1 - A3)^n}$$

Similarly, max confidence can be found by sorting the factors in increasing order and evaluating the same expressions.

R. Murphy, "Dempster-Shafer Theory for Sensor Fusion in Autonomous Mobile Robots," IEEE Trans. Robotics and Automation, vol. 14, no. 2, Apr. 1998.

Belief Function: Example

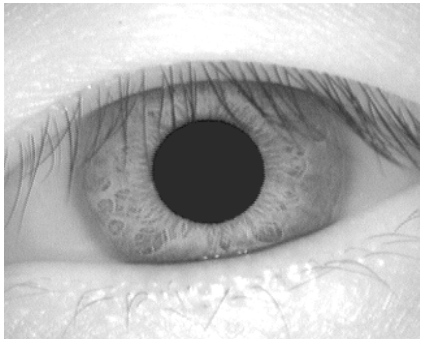

Defocus	Motion Blur	Occlusion	Max Conf.	Min Conf.
0.11524	0.0125	0.45122	.94	.85

- A sample CASIA image, and confidence bounds for image quality.
- Scores are between [0,1] with 0 corresponding to the lowest error and 1 corresponding to highest error.

Defocus	Motion Blur	Occlusion	Max Conf.	Min Conf.
0.68843	0.0125	0.38889	.89	.69

With a bad quality image, the bounds are not tight. The image is characterized by high Occlusion and Defocus blur.

Quality Results

- The metric is tested on CASIA and WVU datasets.
- CASIA data set consists of 108 users with 7 images per user.
- WVU dataset consists of 356 different eyes with 2-18 images per user.
- Rough Segmentation Results

Dataset	Number of Images	Failed Segmentations	Performance
CASIA	756	18	98%
WVU	2495	360	86%

Quality Results

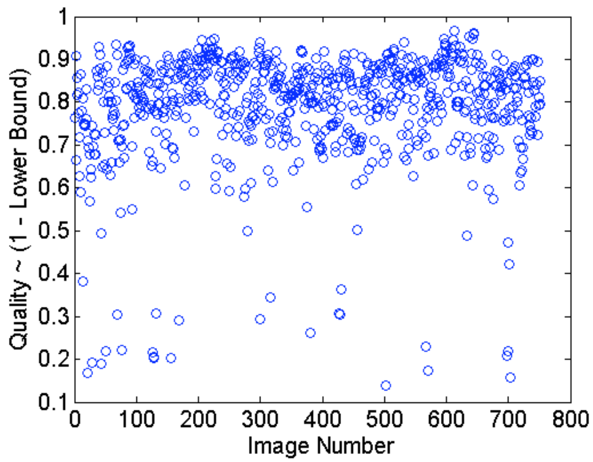

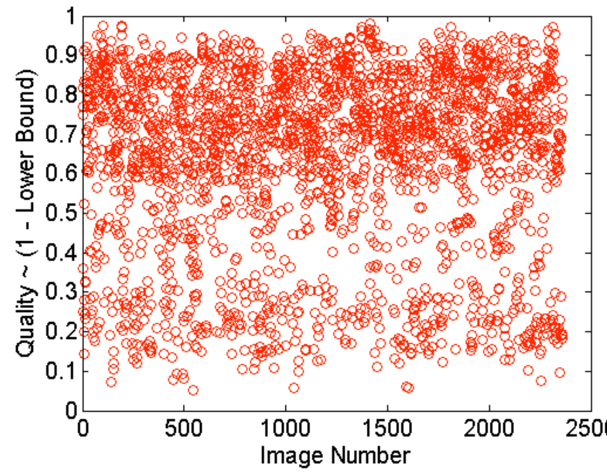

CASIA

Quality per Image

Quality per Image

WVU

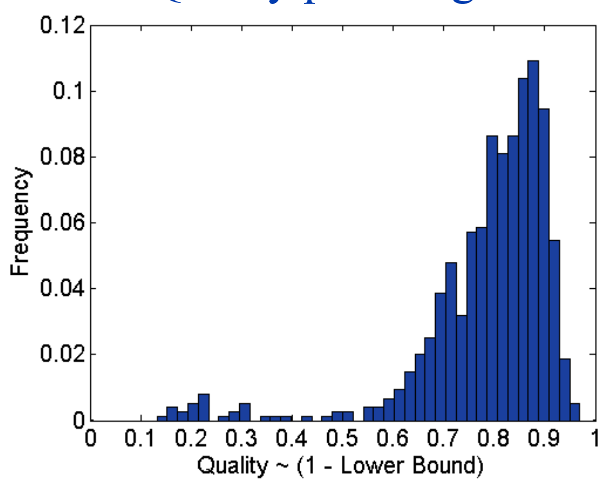

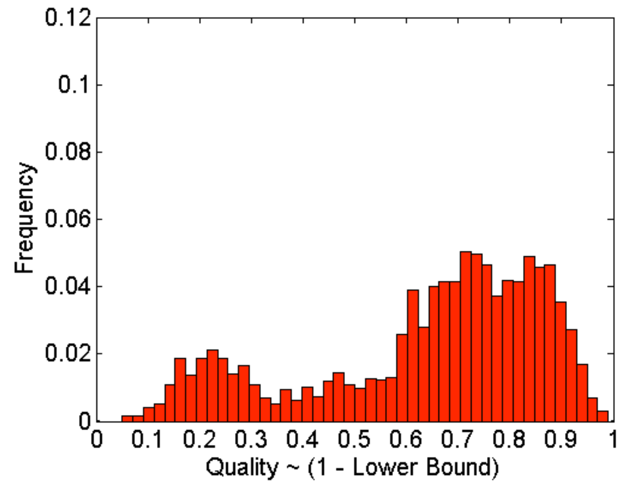

Quality Results: Defocus

Reversed metric: 0 – good quality
1 – poor quality

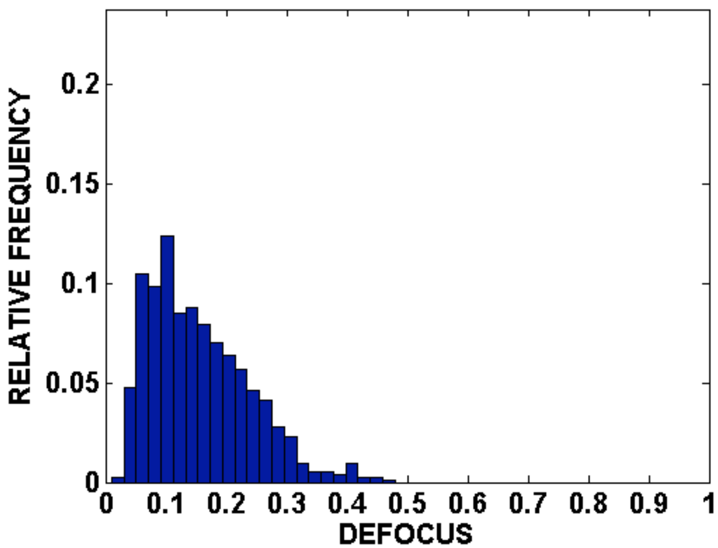

CASIA

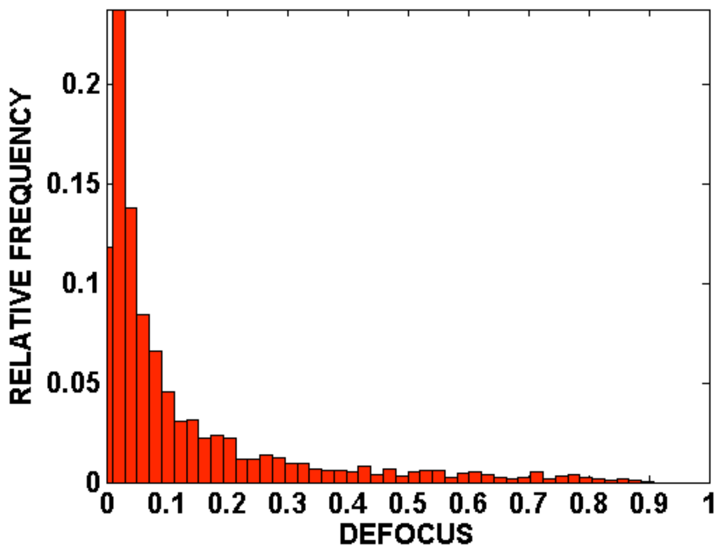

WVU

Motion, Occlusion

CASIA

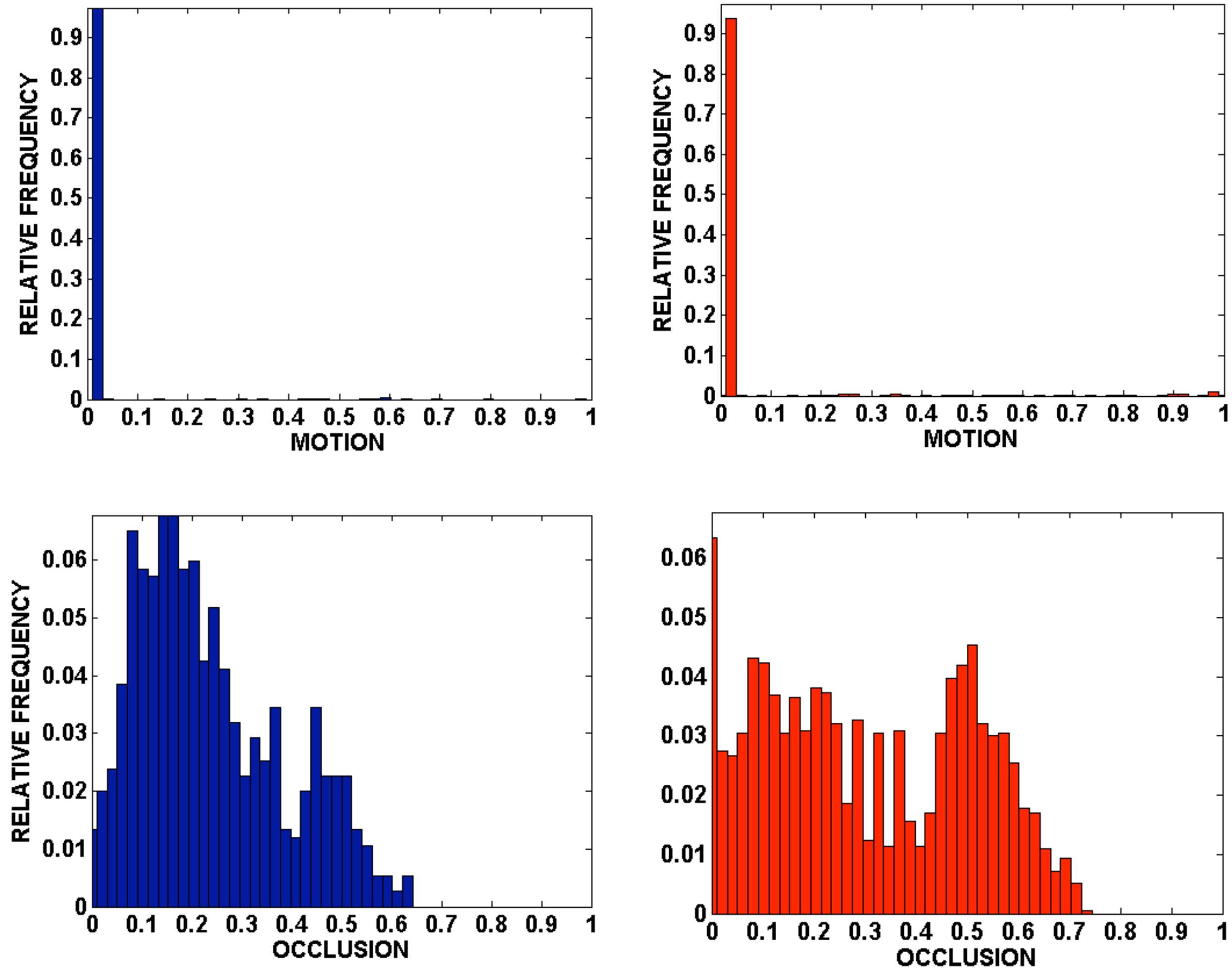

WVU

Lighting, Specular

CASIA

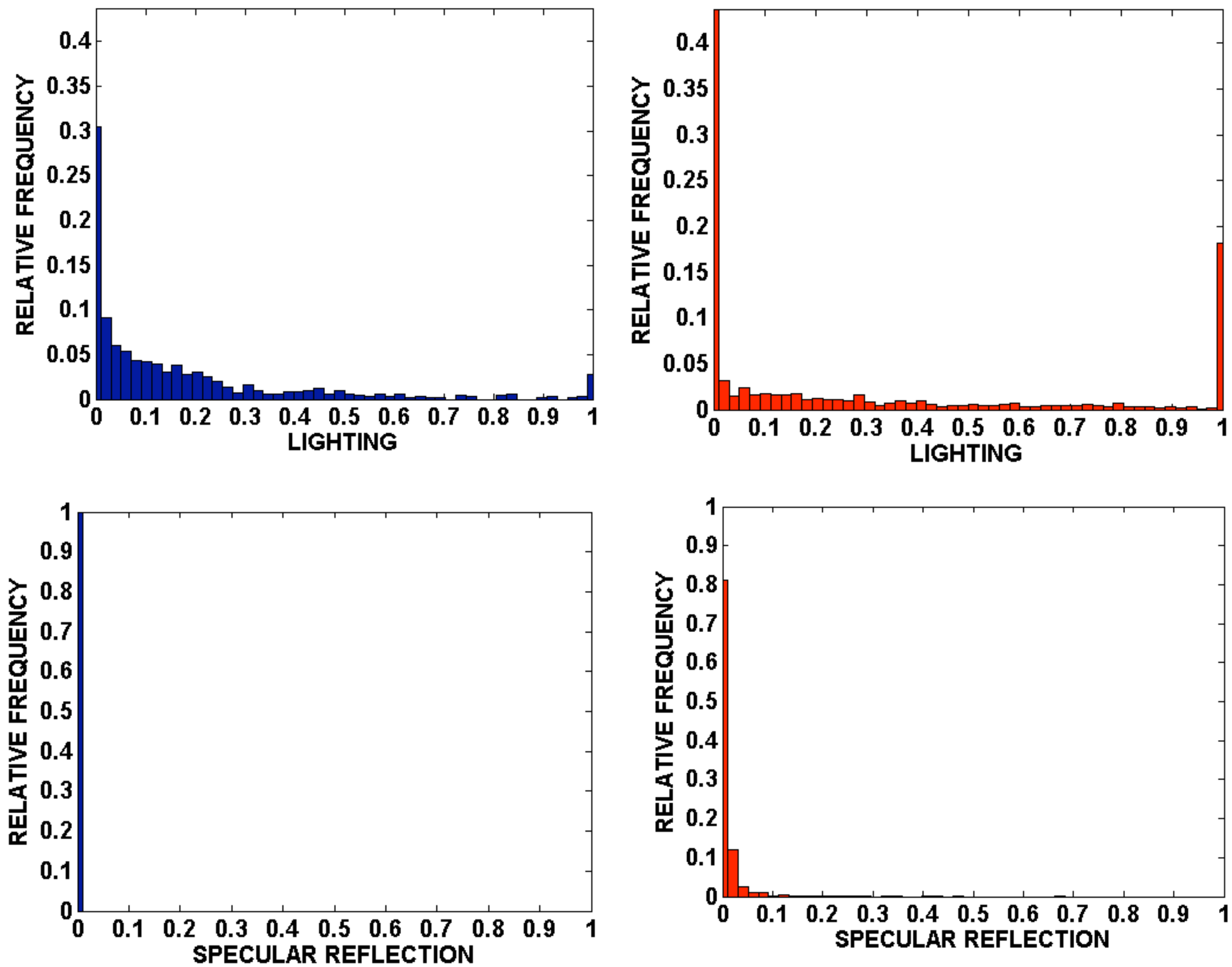

WVU

Pixel Counts

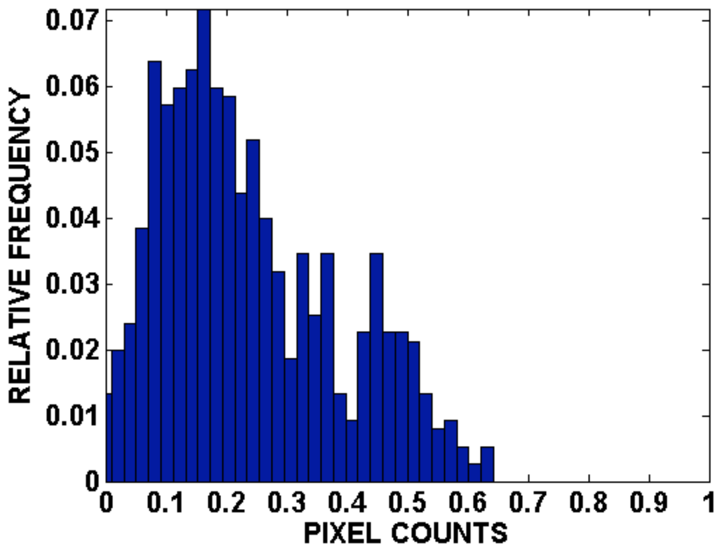

CASIA

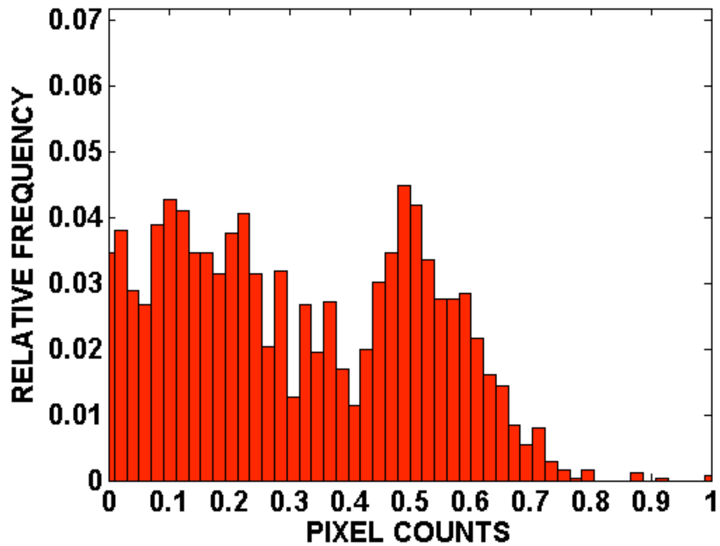

WVU

Performance: Gabor based

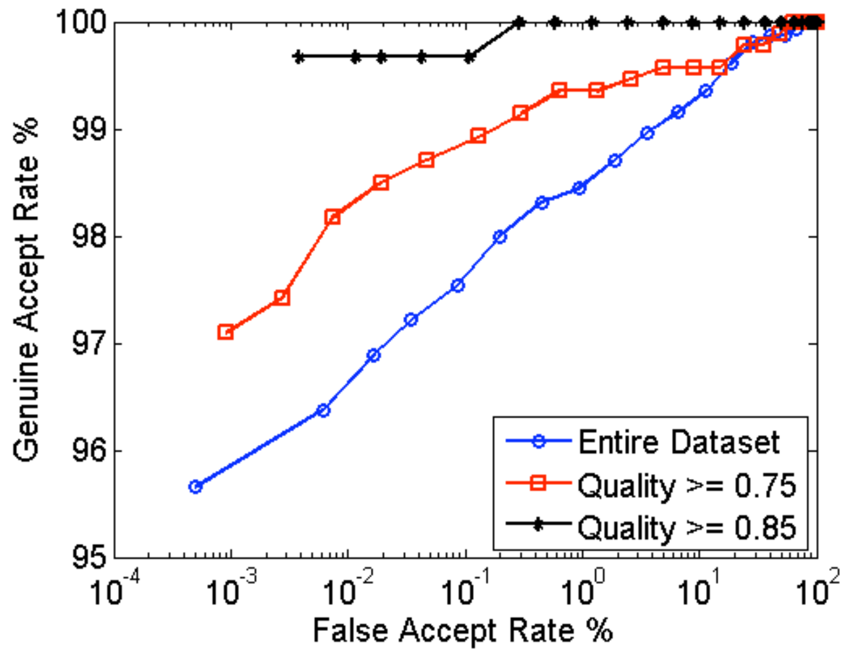

Interval	EER	Dprime	Quality	Images
All	1.30	2.63	0.79	738
Quality $\geq$ 0.75	0.63	2.79	0.85	556
Quality $\geq$ 0.85	0.11	3.13	0.89	273

Performance: Global PCA

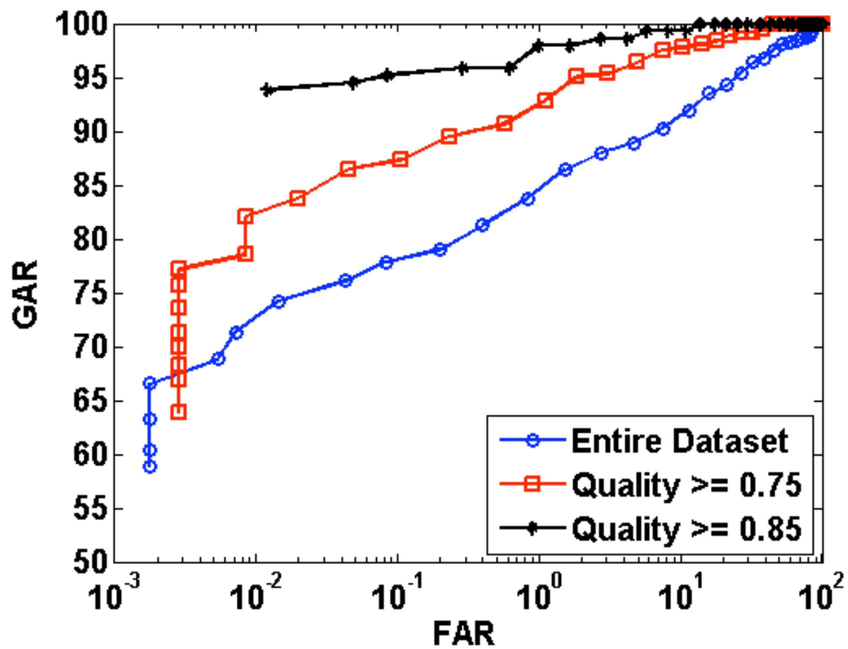

Interval	EER	Dprime	Training	Testing
All	7.51	1.74	108	631
Quality $\geq$ 0.75	3.58	2.14	102	445
Quality $\geq$ 0.85	1.65	2.57	63	186

Performance: Global ICA

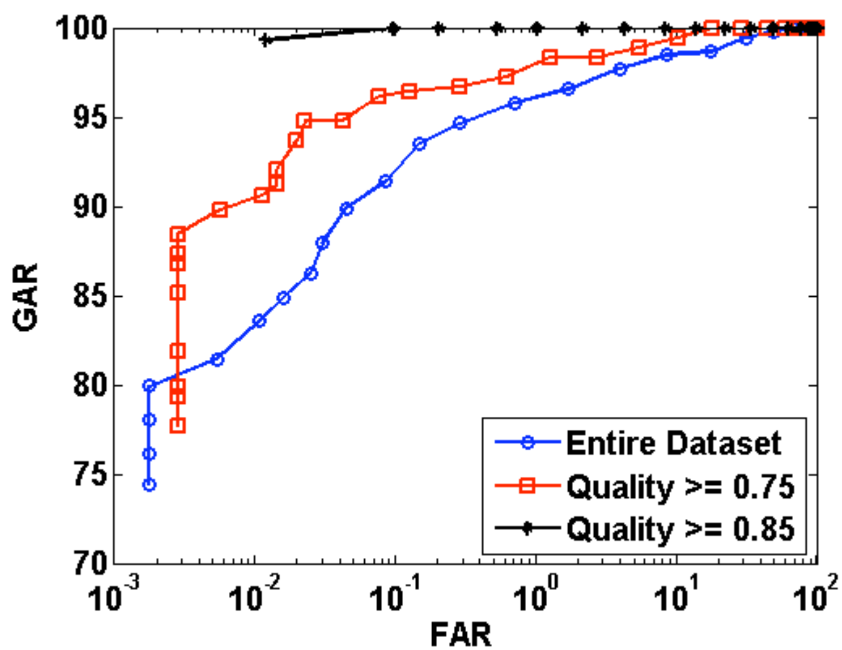

Interval	EER	Dprime	Training	Testing
All	2.29	1.91	108	631
Quality $\geq$ 0.75	1.28	2.23	102	445
Quality $\geq$ 0.85	0.01	2.68	63	186

Performance Comparison

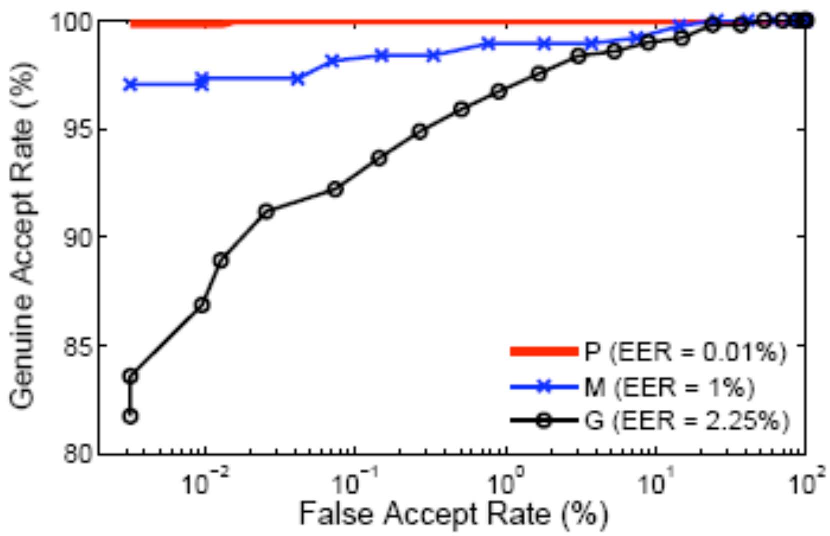

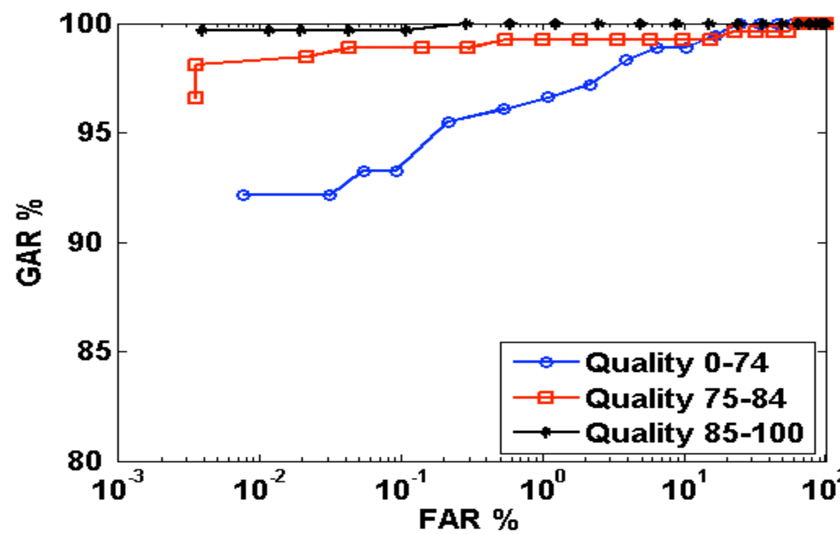

Y. Chen, S. Dass, A. Jain, "Localized Iris Quality Using 2-D Wavelets," in Proc. ICB 2006.

Interval	EER
0-74	2.14
75-84	0.54
85-100	0.11

ICE Phase-I Data

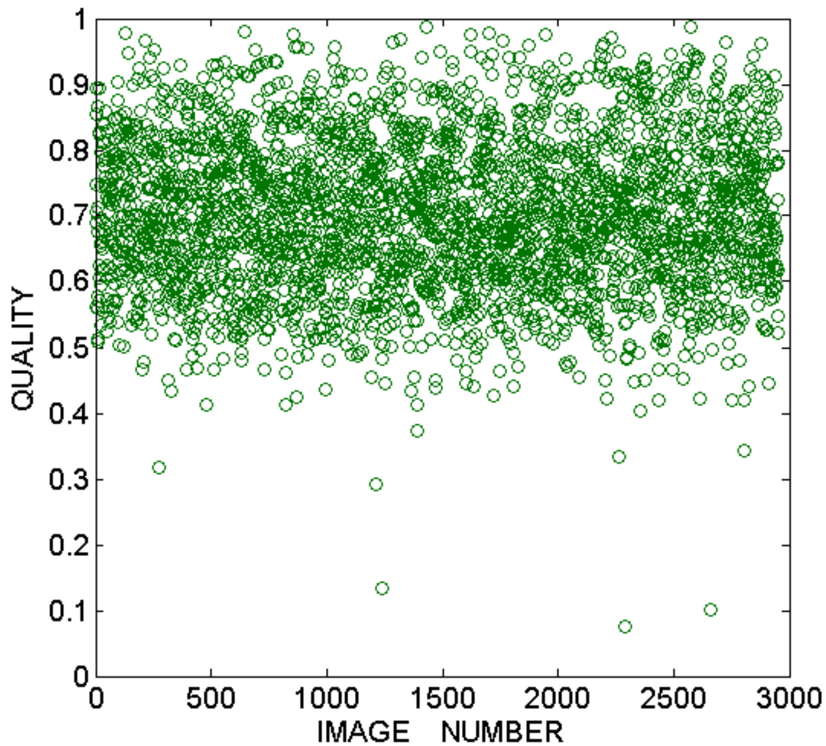

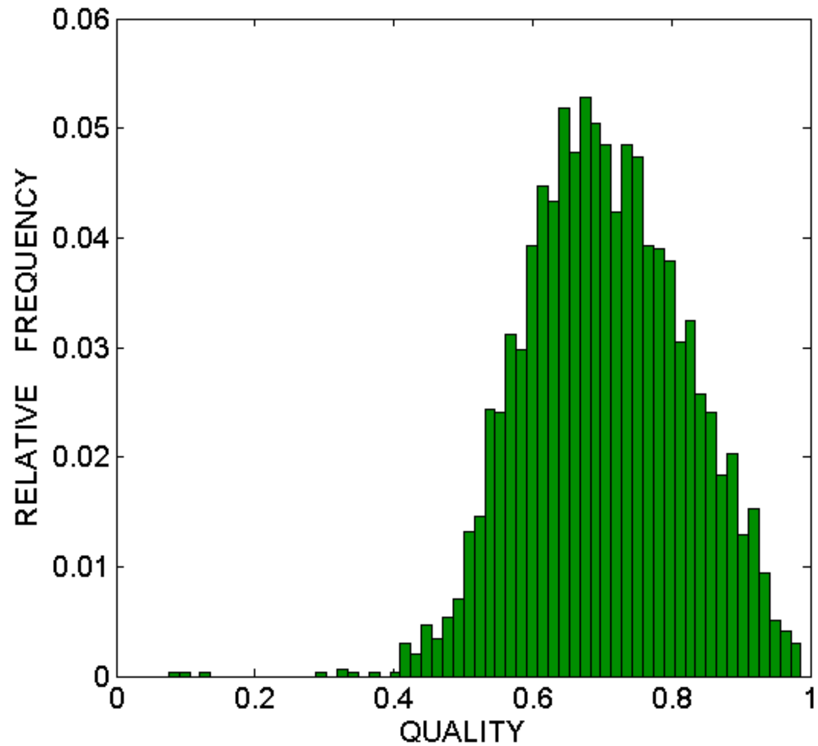

About 2937 iris images

Conclusions

- A metric for Iris image quality metric is developed.
  - It estimates 7 factors: defocus, motion, off-angle, occlusion, lighting, specular, and pixel counts. The factors are fused using Dempster-Shafer theory.
- Only a rough segmentation of iris images is required.
- Quality estimation procedure is efficient in all aspects, with exception of off-angle estimation.
- Performance of our quality metric is comparable to that of Chen et al.

Contact Information

E-mail: Natalia.Schmid@mail.wvu.edu